

An OPF Methodology to Ensure Small-Signal Stability

Rafael Zárate-Miñano, *Student Member, IEEE*, Federico Milano, *Senior Member, IEEE*, and Antonio J. Conejo, *Fellow, IEEE*

Abstract—This paper presents a security redispatching procedure that allows achieving an appropriate security level in terms of small-signal rotor angle stability. The proposed methodology is based on an OPF problem that explicitly considers security limits through stressed loading conditions. The solution of the proposed redispatching procedure yields the optimal preventive control actions to be implemented to ensure a given security level. The New England 39-bus, ten-machine and the IEEE 145-bus, 50-machine systems are used for illustrating, testing, and discussing the proposed technique.

Index Terms—Hopf bifurcation, loading margin, optimal power flow, small-signal rotor angle stability, voltage stability.

NOTATION

The notation used throughout the paper is stated below for quick reference. Throughout the paper, the superscript “A” indicates base-case solution and the superscript “s” indicates stressed operating condition.

A. Functions

z	Objective function.
z_D	Cost function of load active power adjustments.
z_G	Cost function of generation active power adjustments.
z_V	Penalty function of voltage magnitude adjustments.

B. Variables

P_{Di}	Active power consumption of demand i .
P_{Gj}	Active power production of generator j .
Q_{Gj}	Reactive power production of generator j .
V_n	Voltage magnitude at bus n .
$\Delta P_{Di}^{\text{down}}$	Active power decrease in demand i for security purposes.
$\Delta P_{Gj}^{\text{down}}$	Active power decrease in generator j for security purposes.

$\Delta P_{Gj}^{\text{up}}$	Active power increase in generator j for security purposes.
ΔV_n^{down}	Voltage magnitude decrease at bus n for security purposes.
ΔV_n^{up}	Voltage magnitude increase at bus n for security purposes.
θ_n	Voltage angle at bus n .
λ	Loading margin.
λ^*	Optimal loading margin resulting from the OPF problem defined in Appendix A.

C. Eigenvalues

$\alpha \pm j\beta$	Pair of complex eigenvalues associated with the system state matrix.
---------------------	--

D. Constants

c_{Di}^{down}	Cost of decreasing load i for security purposes.
c_{Gj}^{down}	Offering cost of generator j to decrease its dispatched power for security purposes.
c_{Gj}^{up}	Offering cost of generator j to increase its dispatched power for security purposes.
c_{Vn}^{down}	Penalty factor for decreasing voltage magnitude at bus n .
c_{Vn}^{up}	Penalty factor for increasing voltage magnitude at bus n .
$G_k + jB_k$	Series admittance of the branch k connecting buses n and m .
$G_{k0} + jB_{k0}$	Total shunt admittance of the branch k connecting buses n and m .
I_k^{max}	Maximum current magnitude through branch k .
P_{Gj}^{max}	Maximum power output of generator j .
P_{Gj}^{min}	Minimum power output of generator j .
Q_{Gj}^{max}	Reactive power capacity of generator j .
Q_{Gj}^{min}	Minimum reactive power limit of generator j .
R_{Gj}^{up}	Active power ramp-up limit of generator j .

Manuscript received September 29, 2009; revised February 05, 2010, May 10, 2010, and July 28, 2010; accepted September 07, 2010. Paper no. TPWRS-00766-2009.

The authors are with the Electrical Engineering, Department, University of Castilla-La Mancha, Ciudad Real, Spain (e-mail: rafael.zarate@uclm.es; federico.milano@uclm.es; antonio.conejo@uclm.es).

Digital Object Identifier 10.1109/TPWRS.2010.2076838

$R_{G_j}^{\text{down}}$	Active power ramp-down limit of generator j .
ψ_{D_i}	Power factor angle of demand i .
V_n^{max}	Maximum voltage magnitude at bus n .
V_n^{min}	Minimum voltage magnitude at bus n .

E. Parameters

Δt	Time interval considered.
λ^{SM}	Security margin.
ϱ	Probability of the considered operating condition. For the stressed cases, it is the probability of a line outage occurrence.

F. Sets

\mathcal{D}	Set of demands.
\mathcal{D}_n	Set of demands located at bus n .
\mathcal{G}	Set of online generators.
\mathcal{G}_n	Set of online generators located at bus n .
\mathcal{S}	Set of all stressed operating conditions.
\mathcal{S}_u	Subset of stressed operating conditions relevant for small-signal instability analysis ($\mathcal{S}_u \subset \mathcal{S}$).
\mathcal{N}	Set of buses.
\mathcal{N}_G	Set of generator buses.
Ω_k	Set of network branches.
Ω_n	Set of branches connected to bus n .

I. INTRODUCTION

A. Motivation

MOST existing electricity markets have led to a neat separation between the economical analysis (market clearing procedure) and the technical one (security assessment). Furthermore, market participants expect that the security assessment modifies as little as possible the economical dispatch solution. In order to ensure that the security adjustments have the minimum impact on the original market solution, an appropriate approach requires modeling the behavior of the system and the security constraints in detail. As a consequence, the operator typically has to deal with a nonlinear model and advanced stability analysis concepts, such as bifurcation theory. Thus, the security-targeted redispatching step is a complex and not fully solved task. In this vein, the paper focuses on a redispatching procedure that is able to ensure small-signal rotor angle stability while minimizing generally supplier and demand power changes.

B. Literature Review

Small-signal stability is concerned with the ability of a power system to maintain synchronism under small disturbances [1].

Small-signal instability typically appears in the form of rotor angle oscillations whose amplitude increases due to insufficient damping torque. These oscillations can be originated by local modes or by inter-area modes. The former are typically rotor angle oscillations of a single generator swinging against the rest of the system. Damping these oscillations depends on 1) the strength of the transmission system at the generator point of connection, 2) the generator excitation control system, and 3) the generator power output. Inter-area mode oscillations consist in a group of generators swinging against another group of generators. The characteristics of these oscillations are complex and differ significantly from those of local mode oscillations [2]–[4]. Regardless of the local or inter-area nature of the oscillation modes, the small-signal instability is always originated by one or more pair of complex eigenvalues whose real part becomes positive. This phenomenon is known as Hopf bifurcation [5] and has been widely studied in recent years [6]–[9]. Several damping controllers have been proposed to avoid Hopf bifurcations. For example, power system stabilizers (PSS) have proved to be effective in improving small-signal stability. However, damping controllers cannot guarantee that no Hopf bifurcations occurs [10]. As a matter of fact, Hopf bifurcations can have catastrophic consequences on power systems (e.g., the WSCC blackout of August 10, 1996).

Despite the importance of Hopf bifurcations, the consideration of small-signal rotor angle stability constraints in electricity markets is still an open field of research. In [10], the authors propose two sensitivity-based methods to reschedule the generation in order to maximize the power transfer between two areas subject to the small-signal stability constraints under a set of selected contingencies. Both methods use a linear optimization problem in which the amount of active power generation rescheduled in one area is balanced by rescheduling the same amount of active power generation in other area. Contingency filtering is based on the damping ratio of the least stable rotor angle mode in the system [11]. The small-signal stability constraint is formulated in terms of sensitivities of this damping ratio with respect to the active power generation that corresponds to a previously selected set of generators. In [12], the authors include small-signal stability constraints in an optimal power flow (OPF) problem in which the expected security cost, first proposed in [13], is minimized. The OPF problem includes the pre-contingency operating conditions and the post-contingency operating conditions for the entire set of credible contingencies. In [12], the small-signal stability constraints are formulated in terms of the first- and second-order sensitivities of a set of critical eigenvalues with respect to the OPF decision variables. In this paper, small-signal stability constraints are defined based on first-order sensitivities of critical eigenvalues with respect to generator powers.

C. Tool Features and Contributions

This paper improves and extends the security redispatching procedures described in [14] and [15] in order to take into account small-signal stability. The resulting security redispatching procedure allows achieving an appropriate security level in terms of both voltage stability and small-signal stability. The proposed procedure is based on an OPF problem that

includes voltage stability constraints as well as small-signal stability constraints. It has to be noted that the proposed technique serves in those cases where small-signal instability occurs despite existing regulation. In other words, the proposed procedure does not adjust the power productions of market participants instead of using PSS devices, but because the actions of the existing controllers (PSSs included) are not sufficient to provide the system with the required security level.

As in [12], the proposed procedure considers several operating conditions, the adjusted one and a set of stressed operating conditions. The main difference with [12] is that each stressed operating condition is characterized by both a contingency and a fictitious loading level that defines a distance, in terms of load power, to instability and/or collapse. Furthermore, we propose a contingency filtering procedure that allows selecting the very critical contingencies, i.e., a reduced subset of all credible contingencies.

The solution of the proposed redispatching procedure yields the optimal preventive control actions that have to be implemented to ensure a given security margin in terms of small-signal stability. Furthermore, as a byproduct of the proposed OPF problem formulation, voltage stability is also ensured.

D. Paper Organization

The paper is organized as follows. In Section II, the OPF problem is formulated and the steps of the redispatching procedure are described. In Section III, the performance of the proposed procedure is tested using the New England 39-bus, ten-machine system and the IEEE 145-bus, 50-machine system. The results are analyzed and discussed. Finally, Section IV gives some conclusions.

II. SECURITY REDISPATCHING PROCEDURE

This section presents a redispatching procedure based on a small-signal stability constrained optimal power flow (SSSC-OPF) problem to help the independent system operator (ISO) ensure an appropriate security level. We assume that the ISO has access to the technical information of generators and that the generators communicate their offers to the ISO.

The ISO has to ensure that the system operates in safe and stable conditions, including adequate margins with respect to voltage and angle stability. Since small-signal angle stability analysis cannot be performed without the knowledge of technical data (e.g., machine parameters), one has to assume that the ISO has access to such information or, at least, can estimate with reasonable accuracy the required data. As far as we know, ISOs have a reasonable knowledge of the technical data of the system under their control. Furthermore, it is not required that the ISO knows everything of the entire interconnected system. For example, in Europe, the ISO of each country generally has detailed dynamic information only about its national system and has developed adequate static and dynamic equivalents to model the behavior of interconnection buses.

A. SSSC-OPF Problem Description

This subsection describes in detail the objective function and all constraints used in the SSSC-OPF problem. The starting

point of our analysis is the working condition established through a dispatching procedure (e.g., a market clearing algorithm) adjusted by losses in such a way that the voltage profile is optimized. This solution, hereinafter denoted as *base case*, does not typically take into account security. Thus, the ISO has to check whether redispatching actions (that modify the base-case solution) are needed. In the proposed procedure, redispatching does not substitute PSS or any other existing controller actions but, rather, provides additional means to obtain the required stability margin.

1) *Objective Function:* The proposed objective function is aimed at minimizing the variations with respect to the base-case solution. In particular, the objective function is composed of several terms representing adjustment costs and penalty functions. The adjustments correspond to changes on the generated and consumed powers, while the penalty functions concerns voltage magnitudes at generator buses. These terms are as follows:

- 1) The cost function of generation power adjustments is defined as:

$$z_G = \sum_{j \in \mathcal{G}} c_{G_j}^{\text{up}} \Delta P_{G_j}^{\text{up}} + c_{G_j}^{\text{down}} \Delta P_{G_j}^{\text{down}} \quad (1)$$

where $c_{G_j}^{\text{up}}$ and $c_{G_j}^{\text{down}}$ are offering costs provided by suppliers. In practice, these offers can be chosen equal to the generator price offers used in the market clearing procedure, which is solved before the proposed redispatching OPF problem.

- 2) The penalty function of voltage magnitude adjustments at generator buses is

$$z_V = \sum_{n \in \mathcal{N}_G} c_{V_n}^{\text{up}} \Delta V_n^{\text{up}} + c_{V_n}^{\text{down}} \Delta V_n^{\text{down}}. \quad (2)$$

The term (2) is included to penalize the changes on the base-case voltage magnitudes at generator buses since the voltage profile of the base case is considered to be the most suitable one.

- 3) Finally, the cost of adjustments on the demand power decrease is

$$z_D = \sum_{i \in \mathcal{D}} c_{D_i}^{\text{down}} \Delta P_{D_i}^{\text{down}}. \quad (3)$$

To avoid load curtailment unless strictly necessary for maintaining system security, the penalties of voltage magnitude adjustments $c_{V_n}^{\text{up}}$ and $c_{V_n}^{\text{down}}$ are higher than the costs of generation power adjustments $c_{G_j}^{\text{up}}$ and $c_{G_j}^{\text{down}}$ but lower than the costs of load decrease $c_{D_i}^{\text{down}}$. For each considered stressed operating condition, we also include in the objective function a penalty function of the generation power adjustments

$$z_G^s = \sum_{j \in \mathcal{G}} c_{G_j}^{\text{up}} \Delta P_{G_j}^{\text{up},s} + c_{G_j}^{\text{down}} \Delta P_{G_j}^{\text{down},s} \quad (4)$$

and a penalty function of voltage magnitude adjustments

$$z_V^s = \sum_{n \in \mathcal{N}_G} c_{Vn}^{\text{up}} \Delta V_n^{\text{up},s} + c_{Vn}^{\text{down}} \Delta V_n^{\text{down},s}. \quad (5)$$

Terms (4) and (5) are introduced to force all stressed systems to work at an economic operating condition and to maintain appropriate voltage profiles, respectively. However, the cost function of power demand decrease is not considered for the stressed conditions since load powers of the stressed systems are parametrized by the ones of the adjusted one; see (18) and (19) in the next subsection. In summary, the complete objective function is as follows:

$$z = \varrho(z_G + z_V) + z_D + \sum_{s \in \mathcal{S}} \varrho^s (z_G^s + z_V^s) \quad (6)$$

where ϱ and ϱ^s are, respectively, the probability of operating in the adjusted operating condition and the probability of occurrence of the contingency considered in the stressed operating condition s . These probabilities satisfy the condition [13]

$$\varrho + \sum_{s \in \mathcal{S}} \varrho^s = 1 \quad (7)$$

where $\varrho^s \ll \varrho$.

2) *Power Flow Equations for the Adjusted Operating Condition:* The adjusted operating condition of the system is established by the active and reactive power balance at all buses

$$\begin{aligned} & \sum_{j \in \mathcal{G}_n} P_{Gj} - \sum_{i \in \mathcal{D}_n} P_{Di} \\ &= \sum_{k \in \Omega_n} V_n^2 (G_k + 0.5G_{k0}) \\ & \quad - V_n V_m (G_k \cos \theta_{nm} + B_k \sin \theta_{nm}), \quad \forall n \in \mathcal{N} \end{aligned} \quad (8)$$

$$\begin{aligned} & \sum_{j \in \mathcal{G}_n} Q_{Gj} - \sum_{i \in \mathcal{D}_n} P_{Di} \tan(\psi_{Di}) \\ &= \sum_{k \in \Omega_n} -V_n^2 (B_k + 0.5B_{k0}) \\ & \quad - V_n V_m (G_k \sin \theta_{nm} - B_k \cos \theta_{nm}), \quad \forall n \in \mathcal{N} \end{aligned} \quad (9)$$

where $\theta_{nm} = \theta_n - \theta_m$ and with

$$P_{Gj} = P_{Gj}^A + \Delta P_{Gj}^{\text{up}} - \Delta P_{Gj}^{\text{down}}, \quad \forall j \in \mathcal{G} \quad (10)$$

$$P_{Di} = P_{Di}^A - \Delta P_{Di}^{\text{down}}, \quad \forall i \in \mathcal{D} \quad (11)$$

and

$$\Delta P_{Gj}^{\text{up}} \geq 0, \quad \forall j \in \mathcal{G} \quad (12)$$

$$\Delta P_{Gj}^{\text{down}} \geq 0, \quad \forall j \in \mathcal{G} \quad (13)$$

$$\Delta P_{Di}^{\text{down}} \geq 0, \quad \forall i \in \mathcal{D}. \quad (14)$$

The terms on the right-hand side of (8) and (9) are the well-known power flow equations and depend on the bus voltage magnitudes and angles.

The voltage magnitudes at generator buses are defined as

$$V_n = V_n^A + \Delta V_n^{\text{up}} - \Delta V_n^{\text{down}}, \quad \forall n \in \mathcal{N}_G \quad (15)$$

with

$$\Delta V_n^{\text{up}} \geq 0, \quad \forall n \in \mathcal{N}_G \quad (16)$$

$$\Delta V_n^{\text{down}} \geq 0, \quad \forall n \in \mathcal{N}_G. \quad (17)$$

Equation (9) implies that constant power factor loads are considered. Superscript ‘‘A’’, in (10), (11), and (15), indicates base-case solution.

3) *Power Flow Equations for the Stressed Operating Conditions:* The power flow equations for the stressed operating conditions are

$$\begin{aligned} & P_{Gj}^s - \sum_{i \in \mathcal{D}_n} (1 + \lambda^{\text{SM}}) P_{Di} \\ &= \sum_{k \in \Omega_n} (V_n^s)^2 (G_k + 0.5G_{k0}) \\ & \quad - V_n^s V_m^s (G_k \cos \theta_{nm}^s + B_k \sin \theta_{nm}^s), \\ & \quad \forall n \in \mathcal{N}, \forall s \in \mathcal{S} \end{aligned} \quad (18)$$

$$\begin{aligned} & \sum_{j \in \mathcal{G}_n} Q_{Gj}^s - \sum_{i \in \mathcal{D}_n} (1 + \lambda^{\text{SM}}) P_{Di} \tan(\psi_{Di}) \\ &= \sum_{k \in \Omega_n} - (V_n^s)^2 (B_k + 0.5B_{k0}) \\ & \quad - V_n^s V_m^s (G_k \sin \theta_{nm}^s - B_k \cos \theta_{nm}^s), \\ & \quad \forall n \in \mathcal{N}, \forall s \in \mathcal{S} \end{aligned} \quad (19)$$

with

$$P_{Gj}^s = P_{Gj} + \Delta P_{Gj}^{\text{up},s} - \Delta P_{Gj}^{\text{down},s} \quad \forall j \in \mathcal{G}, \forall s \in \mathcal{S} \quad (20)$$

$$\Delta P_{Gj}^{\text{up},s} \geq 0, \quad \forall j \in \mathcal{G}, \quad \forall s \in \mathcal{S} \quad (21)$$

$$\Delta P_{Gj}^{\text{down},s} \geq 0, \quad \forall j \in \mathcal{G}, \quad \forall s \in \mathcal{S} \quad (22)$$

and P_{Di} provided by (11).

The functions of the right-hand side of (18) and (19) have the same expressions as the power flow (8) and (9), respectively, except for substituting the corresponding variables by those pertaining to the stressed operating conditions. The voltage magnitudes at the generator buses are defined as

$$V_n^s = V_n + \Delta V_n^{\text{up},s} - \Delta V_n^{\text{down},s}, \quad \forall n \in \mathcal{N}_G, \forall s \in \mathcal{S} \quad (23)$$

with

$$\Delta V_n^{\text{up},s} \geq 0, \quad \forall n \in \mathcal{N}_G, \quad \forall s \in \mathcal{S} \quad (24)$$

$$\Delta V_n^{\text{down},s} \geq 0, \quad \forall n \in \mathcal{N}_G, \quad \forall s \in \mathcal{S}. \quad (25)$$

Equations (18) and (19) represent the system at the loading level determined by the security margin λ^{SM} . Moreover, (18) and (19) include a single line outage to enforce the $N - 1$ contingency criterion.

4) *Technical Limits*: The power production is limited by the capacity of the generators. Hence, under adjusted and stressed operating conditions

$$P_{G_j}^{\min} \leq P_{G_j} \leq P_{G_j}^{\max}, \quad \forall j \in \mathcal{G} \quad (26)$$

$$P_{G_j}^{\min} \leq P_{G_j}^s \leq P_{G_j}^{\max}, \quad \forall j \in \mathcal{G}, \quad \forall s \in \mathcal{S} \quad (27)$$

$$Q_{G_j}^{\min} \leq Q_{G_j} \leq Q_{G_j}^{\max}, \quad \forall j \in \mathcal{G} \quad (28)$$

$$Q_{G_j}^{\min} \leq Q_{G_j}^s \leq Q_{G_j}^{\max}, \quad \forall j \in \mathcal{G}, \quad \forall s \in \mathcal{S}. \quad (29)$$

A more precise capability curve can be used instead of constraints (26)–(29). However, since detailed dynamic models of generators and automatic voltage regulators are used for determining the small-signal stability constraints, it is not necessary to include a precise capability curve in the OPF problem. Voltages magnitudes throughout the system under the adjusted and the stressed operating conditions should be within operating limits

$$V_n^{\min} \leq V_n \leq V_n^{\max}, \quad \forall n \in \mathcal{N} \quad (30)$$

$$V_n^{\min} \leq V_n^s \leq V_n^{\max}, \quad \forall n \in \mathcal{N}, \quad \forall s \in \mathcal{S}. \quad (31)$$

The current flow through all branches of the network should be below thermal limits

$$\begin{aligned} & \left| 0.5(G_{k0} + jB_{k0})V_n e^{j\theta_n} \right. \\ & \quad \left. + (G_k + jB_k)(V_n e^{j\theta_n} - V_m e^{j\theta_m}) \right| \\ & \leq I_k^{\max}, \quad \forall k \in \Omega_k \end{aligned} \quad (32)$$

$$\begin{aligned} & \left| 0.5(G_{k0} + jB_{k0})V_n^s e^{j\theta_n^s} \right. \\ & \quad \left. + (G_k + jB_k)(V_n^s e^{j\theta_n^s} - V_m^s e^{j\theta_m^s}) \right| \\ & \leq I_k^{\max}, \quad \forall k \in \Omega_k^s, \quad \forall s \in \mathcal{S}. \end{aligned} \quad (33)$$

The changes in the production of generators between adjusted and stressed conditions are limited by ramping constraints

$$P_{G_j}^s - P_{G_j} \leq R_{G_j}^{\text{up}} \Delta t, \quad \forall j \in \mathcal{G}, \quad \forall s \in \mathcal{S} \quad (34)$$

$$P_{G_j} - P_{G_j}^s \leq R_{G_j}^{\text{down}} \Delta t, \quad \forall j \in \mathcal{G}, \quad \forall s \in \mathcal{S} \quad (35)$$

where Δt is a time interval within which generators must be able to adjust their power productions in order to reach the stressed operating conditions. Equation (34) and (35) along with (18) and (19) couple the variables of the stressed operating conditions with those pertaining to the adjusted operating condition. Constraints (34) and (35) enforce the fact that up and down changes of generator powers can be obtained only within given rates, which in turn depends on the type and the characteristics of the

power plants. A further discussion on (34) and (35) and similar ramping constraints can be found in [15].

5) *Small-Signal Stability Constraints*: So far, we have not introduced any differential equation. Actually, we do not include directly differential algebraic equations (DAE) in the proposed SSSC-OPF problem but rather solve an eigenvalue analysis of the state matrix of the system DAE and then define a linear constraint based on eigenvalue sensitivities with respect to generated powers. Only this constraint is included in the SSSC-OPF problem, not the DAE system, which makes the problem tractable. The dynamics that are considered for setting up the system state matrix are synchronous machine transient models (i.e., IV-order models) and AVR controls. These models are described in several books and are not reported here for brevity. The interested reader can find in [16] a complete description of the models and the small-signal stability analysis used in this paper.

The eigenvalues of the system state matrix that are associated with a particular operating condition are implicit nonlinear functions of the system variables and parameters. As it is well-known, small-signal instability occurs if the real part of an eigenvalue (say $\alpha \pm j\beta$) of the system state matrix “moves” from the left-hand side ($\alpha < 0$) to the right-hand side ($\alpha > 0$) of the complex plane, following a parameter variation. Therefore, the small-signal stability boundary is $\alpha = 0$ for all “critical” eigenvalues whose real part is approaching the imaginary axis. It is relevant to note that computing all eigenvalues of a large system may involve a high computational effort. However, we are interested only in a subset of eigenvalues, i.e., those with minimum absolute real part. Thus, efficient numerical methods (e.g., Rayleigh’s iteration) can be used.

The goal of the proposed SSSC-OPF problem is to stabilize the set of stressed operating conditions that shows positive (unstable) eigenvalues. At this aim, we introduce small-signal stability constraints based on the first-order Taylor series expansion of the critical eigenvalue real part, taking into account the dependence of the eigenvalue real part α only on active power generations. In general, eigenvalues are highly nonlinear with respect to system parameters. However, eigenvalues associated with Hopf bifurcations have been shown to vary smoothly with respect to power changes [17].

For the set of unstable stressed operating conditions (\mathcal{S}_u), the small-signal stability constraints are as follows:

$$\alpha^s + F^s \sum_{j \in \mathcal{G}} \sigma_j^s \delta P_{G_j}^s \leq \alpha_{\max}, \quad \forall s \in \mathcal{S}_u \quad (36)$$

where:

- α_{\max} is the limit for the critical eigenvalue real part. This limit can be defined either in terms of the HB point, i.e., $\alpha_{\max} = 0$, or in terms of a minimal damping ratio (ζ_{\min}) as follows:

$$\alpha_{\max} = -\frac{\zeta_{\min} \beta^s}{\sqrt{1 - \zeta_{\min}^2}}, \quad \forall s \in \mathcal{S}_u \quad (37)$$

where β^s is the critical eigenvalue imaginary part.

- σ_j^s is the sensitivity of α^s with respect to changes in the generator power output P_{Gj}^s , i.e.,

$$\sigma_j^s = \left. \frac{\partial \alpha^s}{\partial P_{Gj}^s} \right|_u. \quad (38)$$

- δP_{Gj}^s is a finite variation in the form

$$\delta P_{Gj}^s = P_{Gj}^s - P_{Gj}^{s,u} \quad (39)$$

where $P_{Gj}^{s,u}$ is the active power output of generator j at the unstable stressed operating condition s .

- F^s is a scaling factor that avoids large variations δP_{Gj}^s and, thus, possible infeasibility of the proposed OPF problem.

In this paper, sensitivities (38) are computed using numeric differentiation, i.e., by means of finite small variations of generated powers around the equilibrium point. The procedure is similar to those used in [18] and [19] for computing transmission line sensitivities, and works as follows.

- 1) As a result of the modal analysis carried out in step 4 of the proposed redispatching procedure, the real part α^s of the critical eigenvalue corresponding to a stressed operating condition s is obtained.
- 2) The generator power output P_{Gj}^s is varied of a small quantity, say ϵ , and the modal analysis is performed again. A new value of the critical eigenvalue is obtained whose real part is α_ϵ^s .
- 3) The sensitivity σ_j^s is computed as

$$\sigma_j^s = \frac{\partial \alpha^s}{\partial P_{Gj}^s} \approx \frac{\alpha_\epsilon^s - \alpha^s}{\epsilon}. \quad (40)$$

This procedure is repeated for all generator power outputs of the stressed operating condition considered. The rationale behind the scaling factor F^s in (36) is as follows. Due to nonlinearity, the approximation of the first-order Taylor series expansion can be inaccurate if the power variations δP_{Gj}^s are too large. The size of these variations depends on the relative values of α^s and σ_j^s . Numerical simulations carried out throughout the work reported in this paper show that sensitivities (38) have in general small values (typically an absolute value less than 1), whereas the real part of an eigenvalue can have, in principle, any value. If the difference between the α^s and σ_j^s is relatively large (say, a factor of 10), satisfying (36) can lead to unnecessary large variations of δP_{Gj}^s . Generally, the larger the values of δP_{Gj}^s , the further the solution moves from the initial stressed operating condition. Thus, a weighting factor F^s that allows controlling the size of δP_{Gj}^s is introduced. Since all sensitivities are multiplied by the same constant F^s , the global direction of (36) is not modified as all power variations δP_{Gj}^s are equally scaled. The following formula provides a suitable value for F^s :

$$F^s = \frac{\alpha^s - \alpha_{\max}}{\sigma_{\min}^s \delta \bar{P}} \quad (41)$$

where

$$\sigma_{\min}^s = \min(|\sigma_j^s|), \quad \forall j \in \mathcal{G}, \quad \forall \sigma_j^s \neq 0 \quad (42)$$

and the parameter $\delta \bar{P}$ ($\delta \bar{P} > 0$) is the desired bound for all δP_{Gj}^s , i.e., $|\delta P_{Gj}^s| \leq \delta \bar{P}$.

The purpose of constraint (36) is to drive unstable eigenvalues from the right-hand side to the left-hand side of the imaginary axis of the complex plane. Thus, the smaller is the value of $\delta \bar{P}$, the smaller is typically the variation of α^s .

The statement above can be qualitatively deduced from the following observations.

- 1) The coefficient F^s amplifies the effect of δP_{Gj}^s , i.e., increasing F^s allows satisfying (36) with smaller increments of δP_{Gj}^s .
- 2) Small increments of δP_{Gj}^s lead to a small variation of the current operating point and thus to small changes of the eigenvalues.

Constraints (43) and (44) below are used along with (36) for ensuring that the variations of generator powers are always consistent with the sign of the sensitivities:

$$\delta P_{Gj}^s \geq 0 \quad \text{if} \quad \sigma_j^s < 0, \quad \forall j \in \mathcal{G}, \quad \forall s \in \mathcal{S}_u \quad (43)$$

$$\delta P_{Gj}^s \leq 0 \quad \text{if} \quad \sigma_j^s > 0, \quad \forall j \in \mathcal{G}, \quad \forall s \in \mathcal{S}_u. \quad (44)$$

6) *Other Constraints:* The proposed SSSC-OPF problem includes the following additional constraints:

$$-\pi \leq \theta_n \leq \pi, \quad \forall n \in \mathcal{N} \quad (45)$$

$$-\pi \leq \theta_n^s \leq \pi, \quad \forall n \in \mathcal{N}, \quad \forall s \in \mathcal{S} \quad (46)$$

$$\theta_{\text{ref}} = 0 \quad (47)$$

$$\theta_{\text{ref}}^s = 0, \quad \forall s \in \mathcal{S}. \quad (48)$$

Equations (45) and (46) are included to reduce the feasibility region, thus speeding up eventually the convergence of the OPF problem.

7) *SSSC-OPF Problem Formulation:* The formulation of the SSSC-OPF problem is summarized as follows:

Minimize (6)

subject to

- 1) power flow equations for the adjusted operating condition (8), (9);
- 2) power flow equations for all the stressed operating conditions (18), (19);
- 3) technical limits (26)–(35);
- 4) small-signal stability constraints (36) and (43), (44);
- 5) other constraints (45)–(48).

The optimization variables of the proposed SSSC-OPF problem are: V_n , θ_n , V_n^s , θ_n^s , P_{Gj} , Q_{Gj} , P_{Di} , P_{Gj}^s , Q_{Gj}^s , $\Delta P_{Gj}^{\text{up}}$, $\Delta P_{Gj}^{\text{down}}$, $\Delta P_{Gj}^{\text{up},s}$, $\Delta P_{Gj}^{\text{down},s}$, $\Delta P_{Di}^{\text{down}}$, ΔV_n^{up} , ΔV_n^{down} , $\Delta V_n^{\text{up},s}$, $\Delta V_n^{\text{down},s}$, and δP_{Gj}^s .

B. Security Redispatching Procedure

The proposed OPF problem includes an “adjusted” operating condition as well as a number of “stressed” ones. Each stressed operating condition has to be stable at the desired loading level λ^{SM} . This means that each stressed operating condition has to be both a feasible power flow solution (i.e., voltage stable) and a feasible equilibrium point (i.e., small-signal stable). In other words, we first ensure that the current operating condition is sufficiently far away from voltage instability and then ensure that it is sufficiently far away from small signal instability. Note that without ensuring voltage stability, it is not possible to run an eigenvalue analysis at the equilibrium point, since such equilibrium point would not exist. Hence, the voltage stability is a prerequisite for the small signal stability but is not “coupled” with it.

The proposed security redispatching procedure based on the proposed SSSC-OPF works as follows.

1) *Base-Case Solution.* The base-case solution corresponds to the solution of a dispatching procedure (e.g., a market clearing procedure) adjusted by losses in such a way that the voltage profile is optimized.

2) *Selection of Stressed Operating Conditions.*

For each considered contingency, the loading margin λ^* of the system is computed by means of the maximum loading condition (MLC)-OPF problem described in Appendix A. At the maximum loading condition, an eigenvalue analysis is carried out (see Appendix B). For a given security margin λ^{SM} , the contingency is selected if:

- $\lambda^* < \lambda^{\text{SM}}$. This means that the system exhibits potential voltage instability at the considered loading condition.
- The real part of an eigenvalue at the maximum loading condition is positive. This situation implies that a Hopf bifurcation has occurred. Thus, the system can be subjected to small-signal instability at the required loading condition.

A set of stressed operating condition constraints is included in the SSSC-OPF problem for each selected contingency fixing the value of λ^{SM} in (18) and (19).

3) *Solution of the SSSC-OPF Problem.* The OPF problem described in Section II-A7 is solved, and the adjusted and the stressed operating conditions are computed. The first time that this problem is solved, constraints (36) and (43), (44) are not included.

4) *Eigenvalue Analysis.* An eigenvalue analysis is carried out in order to determine the stability of each stressed operating condition computed in step 3. This analysis requires two preparatory steps: 1) computing the equilibrium point through the initialization of the dynamic devices (e.g., synchronous machines and AVRs); and 2) setting up the system state matrix for that equilibrium point. Regarding the stability of the stressed operating conditions, two scenarios are possible:

- The real part of all eigenvalues associated with all stressed operating conditions are negative. All stressed operating conditions are thus stable and the procedure stops.

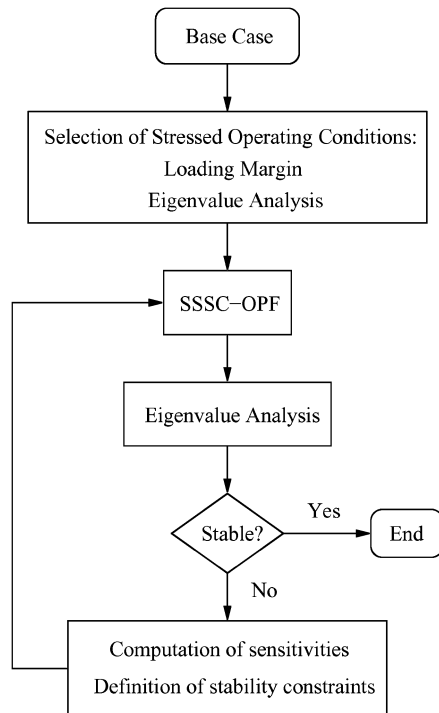


Fig. 1. Flow chart of the proposed procedure.

- One or more stressed operating conditions show an eigenvalue with positive real part. For each one of these contingencies (set \mathcal{S}_u) sensitivities (38) are computed and the constraints (36) and (43), (44) are added to the SSSC-OPF problem. The procedure continues at step 3.

The flowchart depicted in Fig. 1 summarizes the proposed method.

C. Remarks on the Stressed Operating Conditions

How to interpret stressed operating conditions is a delicate issue in any stability-constrained OPF problem that includes a loading parameter (e.g., [20], [21]), which is the case of the proposed SSSC-OPF problem.

It should be noted that the system is not expected to operate at the loading level defined by λ^{SM} . In other words, the load increase represented by λ^{SM} is *not* a predicted load increase. Instead, parameter λ^{SM} is used for enforcing a margin, in load terms, to instability. The value of λ^{SM} is fixed by the ISO. Since each stressed operating condition is defined by a contingency and by the λ^{SM} value, if the system at all the stressed operating conditions is stable, then it is assumed to be stable at the adjusted operating condition as well, and it has at least a margin λ^{SM} to instability even if a contingency occurs.

The small-signal stability constraints are imposed on the stressed operating conditions. These constraints force to change the generator powers in order to ensure small-signal stability at the conditions imposed. In some cases, the changes in the stressed operating conditions imply changes at the adjusted operating condition. This is due to constraints (18), (19) and/or (34), (35), which link the stressed operating conditions to the adjusted one. The changes at the adjusted operating condition

correspond to redispatching actions, or preventive control actions, on the base-case operating condition needed to ensure the desired security margin λ^{SM} .

In other cases, the changes in the stressed operating conditions do not involve any change in the adjusted operating condition. That means that no preventive control actions are needed to achieve the required security margin and the adjusted operating condition remains equal to the base-case one.

A particular case is $\lambda^{\text{SM}} = 0$. In this case, besides the preventive control actions corresponding to the adjusted operating condition, the solution of the proposed procedure provides the emergency control actions needed to maintain stability if any of the considered contingencies occurs. These emergency control actions correspond to the value of the control variables at the different stressed operating conditions.

III. CASE STUDIES

In this section, we consider two benchmark systems, namely the New England 39-bus, ten-machine system and the IEEE 145-bus, 50-machine system. Due to its reduced size, the 39-bus system is particularly well suited for describing the proposed technique. On the other hand, the 145-bus system is used for testing the proposed technique on a comparatively larger system.

A. New England 39-Bus, Ten-Machine System

For this system, generators are modeled using a IV-order model incorporating a primary voltage control, except for generator 10 that represents an equivalent of the New York network (i.e., a large inertia). In order to force small-signal instability, PSS devices are not considered. The full dynamic data of the system can be found in [22] while the base case and the economic and technical data are provided in Appendix C. In this case study, two security margins are considered: $\lambda^{\text{SM}} = 0,07$ and $\lambda^{\text{SM}} = 0,09$.

Neglecting generator islanding, there are 35 possible line outages. Solving the MLC-OPF problem defined in Appendix A and carrying out the eigenvalue analysis, we observe that seven contingencies are characterized by a small-signal unstable maximum loading condition. For the considered security margins, no line outage is selected due to voltage stability issues. Table I provides the loading margin λ^* and the corresponding critical eigenvalues for the seven contingencies selected. In summary, the SSSC-OPF problem used in this case study embodies variables and constraints for the adjusted operating condition and for seven stressed operating conditions.

After solving the first SSSC-OPF problem, two stressed operating conditions show a pair of complex eigenvalues with positive real part for the security margin $\lambda^{\text{SM}} = 0,07$. All stressed operating conditions are stabilized after ten iterations of the proposed procedure using $\delta\bar{P} = 1$ p.u. and $\alpha_{\text{max}} = 0$ in the small-signal stability constraints. Table II provides the critical eigenvalues of the considered stressed operating conditions for

TABLE I
NEW ENGLAND 39-BUS, TEN-MACHINE SYSTEM. LOADING MARGIN AND CRITICAL EIGENVALUES FOR THE SELECTED CONTINGENCIES

Contingency	λ^*	$\alpha \pm j\beta$
1 - 2	0.1004	0.1905 \pm j2.5572
1 - 39	0.1004	0.2089 \pm j2.5518
2 - 25	0.1002	0.2095 \pm j2.7582
8 - 9	0.1006	0.0705 \pm j2.6639
9 - 39	0.1007	0.0922 \pm j2.6590
21 - 22	0.0957	0.7435 \pm j2.4743
28 - 29	0.0976	0.4326 \pm j2.9084

TABLE II
NEW ENGLAND 39-BUS, TEN-MACHINE SYSTEM. CRITICAL EIGENVALUES OF THE STRESSED OPERATING CONDITIONS BEFORE AND AFTER APPLYING THE PROPOSED PROCEDURE FOR $\lambda^{\text{SM}} = 0,07$

Cont.	Iteration 1	Iteration 10
	$\alpha^s \pm j\beta^s$	$\alpha^s \pm j\beta^s$
1 - 2	-0.0350 \pm j2.6911	-0.1580 \pm j2.7349
1 - 39	-0.0206 \pm j2.6725	-0.1631 \pm j2.7043
2 - 25	-0.1605 \pm j2.7804	-0.3038 \pm j2.5579
8 - 9	-0.1451	-0.1449
9 - 39	-0.1477	-0.1476
21 - 22	0.3330 \pm j2.6865	-0.0127 \pm j2.5056
28 - 29	0.2134 \pm j3.0076	-0.1049 \pm j3.0415

the initial unstable solution and for the final stable solution obtained after applying the proposed procedure.

The stressed conditions corresponding to the outage of lines 1–2, 1–39, 2–25, 8–9, and 9–39 become stable after the first iteration.

It is relevant to note that the critical contingencies identified by means of the MLC-OPF problem given in Appendix A are not necessarily unstable at the desired security margin λ^{SM} if $\lambda^* > \lambda^{\text{SM}}$. On the other hand, if for a certain contingency $\lambda^* < \lambda^{\text{SM}}$, that contingency has to be included in the SSSC-OPF problem due to voltage stability and/or security issues. Observe that the proposed procedure is able to take implicitly into account these voltage stability constraints.

For $\lambda^{\text{SM}} = 0,09$, six stressed operating conditions show a pair of complex eigenvalues with positive real part. The stressed condition corresponding to the outage of line 8–9 is stable at the first iteration. All stressed operating conditions are stabilized after 14 iterations of the proposed procedure ($\delta\bar{P} = 1$ p.u. and $\alpha_{\text{max}} = 0$). Table III shows the critical eigenvalues of the considered stressed operating conditions for the initial unstable solution and for the final stable solution after applying the proposed procedure.

Fig. 2 depicts the resulting generation power adjustments $\Delta P_{G_j}^{\text{up}}$ and $\Delta P_{G_j}^{\text{down}}$ needed for ensuring the considered security margins. In both cases, no load curtailment is required. These results show that generation redispatching can be enough to restore small-signal stability. However, for security margins higher than 0.10, load curtailment is needed to stabilize stressed conditions. For example, if the required security margin is $\lambda^{\text{SM}} = 0,11$, all stressed operating conditions are stabilized in one iteration with a total load curtailment of 4.82 p.u.

TABLE III
NEW ENGLAND 39-BUS, TEN-MACHINE SYSTEM. CRITICAL EIGENVALUES
OF THE STRESSED OPERATING CONDITIONS BEFORE AND AFTER
APPLYING THE PROPOSED PROCEDURE FOR $\lambda_{SM} = 0.09$

Contingency	Iteration 1	Iteration 14
	$\alpha^s \pm j\beta^s$	$\alpha^s \pm j\beta^s$
1 - 2	0.1389 ± j2.5837	-0.1032 ± j2.7958
1 - 39	0.1576 ± j2.5766	-0.1018 ± j2.7746
2 - 25	0.1817 ± j2.7639	-0.3902 ± j2.5315
8 - 9	-0.0088 ± j2.6779	-0.3711 ± j2.3574
9 - 39	0.0159 ± j2.6705	-0.3540 ± j2.3731
21 - 22	0.7161 ± j2.4874	-0.0096 ± j2.7604
28 - 29	0.4228 ± j2.9157	-0.2930 ± j3.3282

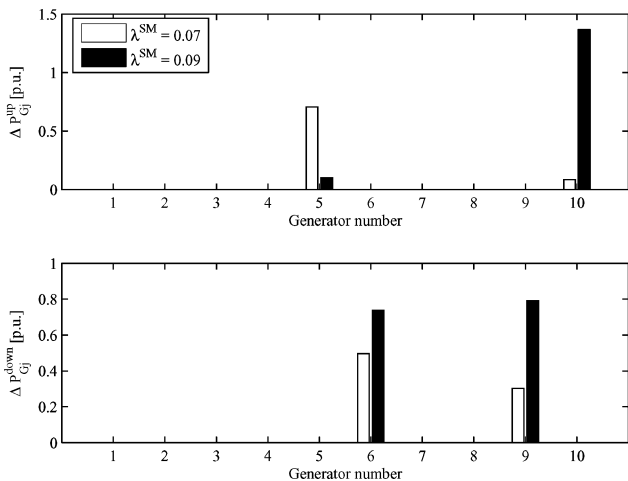


Fig. 2. New England 39-bus, ten-machine system. Redispaching actions needed for ensuring a loading margin $\lambda_{SM} = 0.09$.

TABLE IV
IEEE 145-BUS, 50-MACHINE SYSTEM. LOADING MARGIN AND CRITICAL
EIGENVALUES FOR THE SELECTED CONTINGENCIES

Contingency	λ^*	$\alpha \pm j\beta$
67 - 124	0.0659	0.2165 ± j9.7872
102 - 117	0.0671	0.0702 ± j6.4852
119 - 130	0.0415	-0.0454 ± j9.4041
119 - 131	0.0392	-0.1010 ± j0
121 - 125	0.0521	0.2882 ± j9.5961

B. IEEE 145-Bus, 50-Machine System

We consider a slightly modified version of the IEEE 145-bus, 50-machine benchmark system [23] provided by the software package Power System Toolbox (PST) [24]. This system consists of 145 buses, 453 line/transformers, and 50 machines. Machines connected to buses 93, 102, 104, 105, 106, 110, and 111 are modeled through a VI-order model. These machines are equipped with IEEE ST1a exciters including PSS devices. The classical model is used for the remaining machines. We have removed the PSS device from the machine connected to bus 102 in order to force small-signal instability. The base-case operating condition and dynamic data of this system can be found in [24], whereas economic and technical data are provided in Appendix C.

For this system, 434 possible line/transformer outages are analyzed. In the contingency filtering procedure, the MLC-OPF problem described in Appendix A is solved and an eigenvalue analysis at the maximum loading condition is carried out for each contingency. The desired security margin is set to $\lambda_{SM} = 0.05$. According to the contingency analysis, five contingencies have been considered in the stressed operating conditions. Table IV provides the system loading margin and the critical eigenvalues for these five contingencies. Since the system loading margin λ^* for line 119–130 and 119–131 outages is smaller than the required security margin $\lambda_{SM} = 0.05$, these contingencies can potentially lead to voltage stability issues. On the other hand, line 67–124, 102–117, and 121–125 outages show positive eigenvalues at the maximum loading condition. Thus, these contingencies are selected due to the risk of small-signal instability at the loading condition corresponding to $\lambda_{SM} = 0.05$.

The SSSC-OPF problem for this case study includes variables and constraints for the adjusted operating condition and for five stressed operating conditions. Table V provides the critical eigenvalues of the considered stressed operating conditions for both the initial and the final iteration of the proposed procedure.

The solution of the SSSC-OPF problem without including small-signal stability constraints (first iteration of the proposed procedure) shows generation redispatching and load curtailment. This result is mainly due to the stabilization of the stressed operating conditions corresponding to line 119–130 and 119–131 outages. Note that, for these contingencies, $\lambda^* < \lambda_{SM}$. The load curtailment affects all stressed operating conditions in such a way that the stressed conditions corresponding to line 102–117 and 121–125 outages do not present unstable eigenvalues. However, the stressed operating condition corresponding to line 67–124 outage shows small-signal instability. This stressed operating condition is stabilized in the ninth iteration using $\delta\bar{P} = 1$ p.u. and $\zeta_{min} = 0.05$ in the small-signal stability constraints. The final solution shows a total load curtailment of 2.4078 p.u. Note that standard PSS models are included in VI-order machines, i.e., the full differential-algebraic equations of such controllers have been included in the system model in order to properly compute the state matrix eigenvalues. Thus, PSS actions are implicitly and fully taken into account in the proposed procedure in the same way as generator and AVR models are.

Fig. 3 depicts two time-domain simulations of the 145-bus system at the stressed operating condition corresponding to line 64–124 outage when subjected to a small disturbance. In particular, Fig. 3 shows the unstable rotor speed trajectories for the solution of the first iteration and the stable transient for the final solution of the proposed method. Time-domain simulations confirm eigenvalue analysis.

C. Simulation Times

All simulations presented in this paper have been carried out using Matlab 7.6 [25] and GAMS 22.7 [26], in a Sun Fire X4600 M2, with eight quad-core processors clocking at 2.9 GHz and 256 GB of RAM memory. For solving power flows, eigenvalue analysis, and time-domain simulations, PSAT

TABLE V
IEEE 145-BUS, 50-MACHINE SYSTEM. CRITICAL EIGENVALUES
OF THE STRESSED OPERATING CONDITIONS BEFORE AND AFTER
APPLYING THE PROPOSED PROCEDURE

Contingency	Iteration 1 $\alpha^s \pm j\beta^s$	Iteration 9 $\alpha^s \pm j\beta^s$
67 - 124	0.2740 ± j9.7602	-0.5177 ± j9.3964
102 - 117	-0.1009 ± j0	-0.1009 ± j0
119 - 130	-0.1009 ± j0	-0.1009 ± j0
119 - 131	-0.1010 ± j0	-0.1010 ± j0
121 - 125	-0.1010 ± j0	-0.1010 ± j0

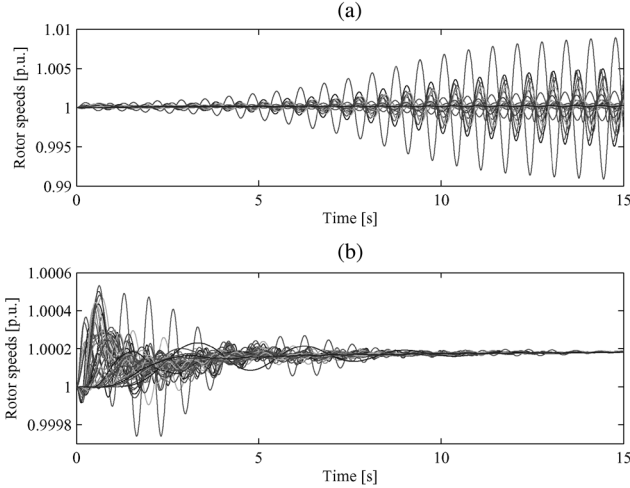


Fig. 3. IEEE 145-bus 50-machine system. Time-domain simulation of the stressed operating condition corresponding to line 64–124 outage. Plot (a) corresponds to the first solution and plot (b) to the final solution.

[27] has been used. All OPF problems has been solved using CONOPT [28] under GAMS.

Each iteration of the proposed procedure involves eigenvalue analysis, computing sensitivities, and solving the SSSC-OPF problem. Eigenvalue analysis is performed for each stressed operating condition obtained after solving the SSSC-OPF problem. Sensitivities of the critical eigenvalue real part with respect to each generator power output are computed by means of numerical differentiation, as described in Section II-A5. Computing sensitivities implies an additional eigenvalue analysis and to evaluate expression (40) for each generator and for each small-signal unstable stressed operating condition. Once sensitivities are computed, the corresponding sets of constraints (36) and (43), (44) are included in the SSSC-OPF problem to be solved. Table VI provides the average step and the total CPU times for the simulations based on the 39-bus and on the 145-bus system. Simulation times for the 39-bus system refers to the simulation for $\lambda^{\text{SM}} = 0.09$.

The proposed procedure comprises some steps that are time consuming, potentially making their implementation impractical for large-scale power systems. This is the case of the eigenvalue analysis and the sensitivity computation. The computational burden of the eigenvalue analysis can be reduced computing only the critical eigenvalues (e.g., using Rayleigh's iteration method). For simplicity, sensitivities have been computed using numerical differentiation. Depending on the system size,

TABLE VI
COMPUTATIONAL REQUIREMENTS OF THE PROCEDURE ITERATIONS

Step	39-bus system		145-bus system	
	Average CPU [s]	Total CPU [s]	Average CPU [s]	Total CPU [s]
Eigen. Analysis	0.04	4.20	0.29	13.05
Sensitivities	0.18	148.84	0.68	270.06
SSSC-OPF	0.31	4.34	54.57	491.14
Total CPU [s]	-	157.38	-	774.25

numerical differentiation may entail a non-negligible computational burden. However, as the sensitivity computations are independent of each other, the required CPU time can be reduced using parallel computation techniques. Alternatively, closed formulas for computing sensitivities reduce significantly the computational burden. These formulas can be found, for instance, in [29]–[32]. Since this paper focuses on the design of an effective procedure, these computational issues have not been specifically addressed.

IV. CONCLUSIONS

This paper presents a security redispatching procedure able to resolve stability issues pertaining to both voltage stability and small-signal stability. It is intended to help system operators guarantee an appropriate level of security for the operation of the system. The proposed procedure provides the optimal redispatching actions on the base-case solution that allow ensuring the required security margin.

The proposed procedure is able to incorporate the $N - 1$ security criterion. In order to reduce the size of the resulting OPF problem, a prior contingency filtering is used for reducing the size of the SSSC-OPF problem, thus incorporating only contingencies that threaten system stability.

Another advantage of the proposed technique is the fact that the redispatching procedure is separated from the small-signal stability analysis, which allows maintaining the OPF problem tractable and structurally similar to existing redispatching problems. Simulation results show the effectiveness of the proposed procedure. Future work will focus on the development of a specific solution algorithm for the proposed SSSC-OPF problem to speed up computations.

APPENDIX A

DETERMINATION OF THE MAXIMUM LOADING CONDITION

In this Appendix, we define the problem for computing the maximum loading condition point that is used in the step 2 of the proposed procedure, as follows:

$$\text{Minimize} \quad -\lambda \quad (49)$$

subject to

$$\begin{aligned} \sum_{j \in \mathcal{G}_n} P_{Gj} - (1 + \lambda) \sum_{i \in \mathcal{D}_n} P_{Di}^A &= \sum_{k \in \Omega_n} V_n^2 (G_k + 0.5G_{k0}) \\ &- V_n V_m (G_k \cos \theta_{nm} + B_k \sin \theta_{nm}), \quad \forall n \in \mathcal{N} \end{aligned} \quad (50)$$

$$\begin{aligned} \sum_{j \in \mathcal{G}_n} Q_{Gj} - (1 + \lambda) \sum_{i \in \mathcal{D}_n} Q_{Di}^A &= \sum_{k \in \Omega_n} -V_n^2 (B_k + 0.5B_{k0}) \\ &- V_n V_m (G_k \sin \theta_{nm} - B_k \cos \theta_{nm}), \quad \forall n \in \mathcal{N} \end{aligned} \quad (51)$$

$$P_{Gj} - P_{Gj}^A \leq R_{Gj}^{\text{up}} \Delta t, \quad \forall j \in \mathcal{G} \quad (52)$$

$$P_{Gj}^A - P_{Gj} \leq R_{Gj}^{\text{down}} \Delta t, \quad \forall j \in \mathcal{G} \quad (53)$$

and constraints (26), (28), (30), (32), (45), and (47).

The superscript “A” denotes base case. Constraints (50), (51) represent the power flow equations with inclusion of one line outage, whereas (52), (53) represent the generators ramp up and ramp down limits, respectively, for the considered time period Δt .

Since in the optimization problem above we use only static equations (i.e., power flow equations), the resulting λ^* does not take into account Hopf bifurcations. Thus, an eigenvalue analysis of the system at the loading level defined by λ^* is carried out separately, including generator dynamic models.

APPENDIX B

SECURITY ASSESSMENT: CONTINGENCY FILTERING

This section describes the procedure used for identifying the harmful contingencies related to small-signal instability as well as to voltage instability. The initial set of contingencies includes all contingencies of the $N - 1$ security criterion, that is, a single outage of any system element. For a given security margin λ^{SM} , the contingency screening procedure works as follows:

- 1) For each one of the initial set of contingencies, the maximum loading condition and the loading margin λ^* of the system are computed using the problem described in Appendix A.
- 2) At the maximum loading condition, a modal analysis is carried out and the eigenvalue with the largest real part α is computed.
- 3) If $\lambda^* \leq \lambda^{\text{SM}}$, the contingency is selected. At the loading condition defined by λ^{SM} , the system exhibits potential voltage instability.
- 4) If $\alpha \geq 0$, the contingency is selected. This situation implies that a Hopf bifurcation has occurred. Thus, at the loading condition defined by λ^{SM} , the system may suffer small-signal instability.
- 5) If $\lambda^* > \lambda^{\text{SM}}$ and $\alpha < 0$, the contingency is filtered out.

Note that the computation of λ^* for one contingency and the modal analysis at the corresponding maximum loading condition are independent of other contingencies. This fact can be exploited for reducing CPU time using parallel computation.

APPENDIX C

SYSTEM DATA

This Appendix provides economic data and technical limits used in the case studies presented in Section III. For both the 39-bus and the 145-bus systems, the considered time period is set to $\Delta t = 5$ minutes and the probability of the occurrence of each selected contingency is $\varrho^s = 0.01$. The units of penalty factors are introduced only for compatibility with costs.

A. New England 39-Bus, Ten-Machine System

Table VII provides the generated active powers and voltage magnitudes at the generator buses for the base case, the offering costs of generators for redispatching purposes, and generator limits. With respect to the offering costs, $c_{Gj}^{\text{up}} = c_{Gj}^{\text{down}}$ for all

TABLE VII
GENERATOR DATA FOR THE NEW ENGLAND 39-BUS, TEN-MACHINE SYSTEM

Gen. #	P_{Gj}^A [p.u.]	V_n^A [p.u.]	c_{Gj}^{down} [$\frac{\$}{\text{p.u.h}}$]	P_{Gj}^{max} [p.u.]	Q_{Gj}^{max} [p.u.]	R_{Gj}^{down} [$\frac{\text{p.u.}}{\text{min.}}$]
1	2.9134	1.0433	6.9	4.025	2.4945	0.0671
2	5.9783	1.05	3.7	7.475	4.6326	0.1246
3	7.8748	1.05	2.8	9.200	5.7016	0.1533
4	7.3089	1.05	4.7	8.625	5.3453	0.1437
5	5.7801	1.05	2.8	7.475	4.6326	0.1246
6	7.4560	1.05	3.7	8.625	5.3453	0.1437
7	6.4704	1.05	4.8	8.625	5.3453	0.1437
8	6.1246	1.05	3.6	8.050	4.9889	0.1342
9	9.4772	1.05	3.7	10.350	6.4144	0.1725
10	11.2828	1.05	3.9	13.800	8.5525	0.2300

generators. With respect to generator limits, $P_{Gj}^{\text{min}} = 0$, $Q_{Gj}^{\text{min}} = -Q_{Gj}^{\text{max}}$ and $R_{Gj}^{\text{up}} = R_{Gj}^{\text{down}}$ for all generators. With regard to bus voltage magnitude limits, $V_n^{\text{max}} = 1.05$ p.u. and $V_n^{\text{min}} = 0.95$ p.u. for all generator buses, and $V_n^{\text{max}} = 1.1$ p.u. and $V_n^{\text{min}} = 0.9$ p.u. for the remaining buses.

The load has been increased by 15% with respect to the base case shown in [22]. For all loads, cost of decreasing load, c_{Di}^{down} , is \$1000/p.u.h, and for all generator buses, costs of increasing and decreasing voltage magnitude, c_{Vn}^{up} and c_{Vn}^{down} , is \$100/p.u.h

B. IEEE 145-Bus, 50-Machine System

Technical limits, offering costs and penalty factors used for the 145-bus system, are as follows. Bus voltage magnitude limits are $V_n^{\text{max}} = 1.1$ p.u. and $V_n^{\text{min}} = 0.9$ p.u. for all generator buses, and $V_n^{\text{max}} = 1.2$ p.u. and $V_n^{\text{min}} = 0.8$ p.u. for the remaining buses. $P_{Gj}^{\text{min}} = 0$ is used for all generators, whereas P_{Gj}^{max} is set to the value that results from increasing the base-case active power output of each generator by 10%. Ramping limits are $R_{Gj}^{\text{up}} = R_{Gj}^{\text{down}} = (P_{Gj}^{\text{max}} - P_{Gj}^{\text{min}})/60$ p.u./min. Generator reactive power limits are provided in [23]. With regard to the offering costs and penalty factors, we use $c_{Gj}^{\text{up}} = c_{Gj}^{\text{down}} = \$10/\text{p.u.h}$ for all generators, $c_{Di}^{\text{down}} = \$1000/\text{p.u.h}$ for all loads, and $c_{Vn}^{\text{up}} = c_{Vn}^{\text{down}} = \$100/\text{p.u.h}$ for all generator buses.

REFERENCES

- [1] IEEE/CIGRE Joint Task Force on Stability Terms and Definitions, “Definition and classification of power system stability,” *IEEE Trans. Power Syst.*, vol. 19, no. 2, pp. 1387–1401, May 2004.
- [2] P. Kundur, *Power System Stability and Control*. New York: McGraw-Hill, 1994.
- [3] IEEE PES Working Group on System Oscillations, Power System Oscillations, IEEE Special Publication 95-TP-101, 1995.
- [4] G. Rogers, *Power System Oscillations*. Boston, MA: Springer, 1999.
- [5] C. A. Cañizares, Voltage Stability Assessment: Concepts, Practices and Tools, IEEE/PES Power System Stability Subcommittee, Tech. Rep. SP101PSS, Aug. 2002.
- [6] H. G. Kwatny and G. E. Piper, “Frequency domain analysis of Hopf bifurcations in electric power systems,” *IEEE Trans. Circuits Syst.*, vol. 37, no. 10, pp. 1317–1321, Oct. 1990.
- [7] C. D. Vournas, M. A. Pai, and P. W. Sauer, “The effect of automatic voltage regulation on the bifurcation evolution in power systems,” *IEEE Trans. Power Syst.*, vol. 11, no. 4, pp. 1683–1688, Nov. 1996.

- [8] C. A. Cañizares, N. Mithulananthan, F. Milano, and R. John, "Linear performance indices to predict oscillatory stability problems in power systems," *IEEE Trans. Power Syst.*, vol. 19, no. 2, pp. 1104–1114, May 2004.
- [9] X. Wen and V. Ajjarapu, "Application of a novel eigenvalue trajectory tracing method to identify both oscillatory stability margin and damping margin," *IEEE Trans. Power Syst.*, vol. 21, no. 2, pp. 817–824, May 2006.
- [10] C. Y. Chung, L. Wang, F. Howell, and P. Kundur, "Generation rescheduling methods to improve power transfer capability constrained by small-signal stability," *IEEE Trans. Power Syst.*, vol. 19, no. 1, pp. 524–530, Feb. 2004.
- [11] L. Wang, F. Howell, P. Kundur, C. Y. Chung, and W. Xu, "A tool for small-signal security assessment of power systems," in *Proc. Int. Conf. Power Industrial Computer. Applications*, Australia, May 2001, pp. 21–24.
- [12] J. Condren and T. W. Gedra, "Expected-security cost optimal power flow with small-signal stability constraints," *IEEE Trans. Power Syst.*, vol. 21, no. 4, pp. 1736–1743, Nov. 2006.
- [13] J. Condren, T. W. Gedra, and P. Damrongkulkamjorn, "Optimal power flow with expected security cost," *IEEE Trans. Power Syst.*, vol. 21, no. 2, pp. 541–547, May 2006.
- [14] A. J. Conejo, F. Milano, and R. Garcia-Bertrand, "Congestion management ensuring voltage stability," *IEEE Trans. Power Syst.*, vol. 21, no. 1, pp. 357–364, Feb. 2006.
- [15] R. Zárate-Miñano, A. J. Conejo, and F. Milano, "OPF-based security redispatching including FACTS devices," *IET Gen., Transm., Distrib.*, vol. 2, no. 6, pp. 821–833, Nov. 2008.
- [16] P. W. Sauer and M. A. Pai, *Power System Dynamics and Stability*. Upper Saddle River, NJ: Prentice-Hall, 1998.
- [17] C. A. Cañizares, N. Mithulananthan, F. Milano, and J. Reeve, "Linear performance indices to predict oscillatory stability problems in power systems," *IEEE Trans. Power Syst.*, vol. 19, no. 2, pp. 1104–1114, May 2004.
- [18] F. Milano, C. A. Cañizares, and M. Invernizzi, "Voltage stability constrained OPF market models considering N-1 contingency criteria," *Elect. Power Syst. Res.*, vol. 74, no. 1, pp. 27–36, Apr. 2005.
- [19] C. A. Cañizares, C. Cavallo, M. Pozzi, and S. Corsi, "Comparing secondary voltage regulation and shunt compensation for improving voltage stability and transfer capability in the Italian power system," *Elect. Power Syst. Res.*, vol. 73, no. 1, pp. 67–76, Jan. 2005.
- [20] F. Milano, C. A. Cañizares, and M. Invernizzi, "Multiobjective optimization for pricing system security in electricity markets," *IEEE Trans. Power Syst.*, vol. 18, no. 2, pp. 596–604, May 2003.
- [21] W. D. Rosehart, C. A. Cañizares, and V. Quintana, "Multiobjective optimal power flows to evaluate voltage security costs in power networks," *IEEE Trans. Power Syst.*, vol. 18, no. 2, pp. 578–587, May 2003.
- [22] M. A. Pai, *Energy Function Analysis for Power System Stability*. Norwell, MA: Kluwer, 1989.
- [23] IEEE Stability Test Systems Task Force of the Dynamic System Performance Subcommittee, "Transient stability test systems for direct stability methods," *IEEE Trans. Power Syst.*, vol. 7, no. 1, pp. 37–43, Feb. 1992.
- [24] Power System Toolbox Ver. 2.0: Dynamic Tutorial and Functions, Cherry Tree Scientific Software. Colborne, ON, Canada, 1999.
- [25] The MathWorks, Inc., Matlab Programming, 2005. [Online]. Available: <http://www.mathworks.com>.
- [26] A. Brooke, D. Kendrick, A. Meeraus, R. Raman, and R. E. Rosenthal, GAMS, a User's Guide, GAMS Development Corp.. Washington, DC, Dec. 1998. [Online]. Available: <http://www.gams.com/>.
- [27] F. Milano, "An open source power system analysis toolbox," *IEEE Trans. Power Syst.*, vol. 20, no. 3, pp. 1199–1206, Aug. 2005.
- [28] A. S. Drud, GAMS/CONOPT, ARKI Consulting and Development, Bagsvaerdvej 246A, DK-2880. Bagsvaerd, Denmark, 1996. [Online]. Available: <http://www.gams.com/>.
- [29] J. E. Van Ness, J. M. Boyle, and F. P. Imad, "Sensitivities of large, multiple-loop control systems," *IEEE Trans. Autom. Control*, vol. 10, no. 3, pp. 308–315, Jul. 1965.
- [30] H. M. Zein El-Din and R. T. H. Alden, "Second order eigenvalue sensitivities applied to power system dynamics," *IEEE Trans. Power App. Syst.*, vol. PAS-96, no. 6, pp. 1928–1936, Nov. 1977.
- [31] T. Smed, "Feasible eigenvalue sensitivity for large power systems," *IEEE Trans. Power Syst.*, vol. 8, no. 2, pp. 555–563, May 1993.
- [32] H. K. Nam, Y. K. Kim, K. S. Shim, and K. Y. Lee, "A new eigen-sensitivity theory of augmented matrix and its applications to power system stability analysis," *IEEE Trans. Power Syst.*, vol. 15, no. 1, pp. 363–369, Feb. 2000.



Rafael Zárate-Miñano (S'05) received the Elect. Eng. degree and the Ph.D. degree from the University of Castilla-La Mancha, Ciudad Real, Spain, in 2005 and 2010, respectively.

He is currently a lecturer at the University of Castilla-La Mancha, Almadén, Spain. His research interests are stability, electricity markets, sensitivity analysis, optimization, and numerical methods.



Federico Milano (SM'09) received the Electrical Engineering and Ph.D. degrees from the University of Genoa, Genoa, Italy, in 1999 and 2003, respectively.

From 2001 to 2002, he worked at the University of Waterloo, Waterloo, ON, Canada, as a Visiting Scholar. He is currently an Associate Professor at the University of Castilla-La Mancha, Ciudad Real, Spain. His research interests include voltage stability, electricity markets, and computer-based power system modeling and analysis.



Antonio J. Conejo (F'04) received the M.S. degree from the Massachusetts Institute of Technology, Cambridge, in 1987, and the Ph.D. degree from the Royal Institute of Technology, Stockholm, Sweden, in 1990.

He is currently a full Professor at the Universidad de Castilla-La Mancha, Ciudad Real, Spain. His research interests include control, operations, planning, and economics of electric energy systems, as well as statistics and optimization theory and its applications.